Improvement in Solid-State Dye Sensitized Solar Cells by p-Type Doping with Lewis Acid SnCl4

ARTICLE *in* THE JOURNAL OF PHYSICAL CHEMISTRY C · OCTOBER 2013

Impact Factor: 4.77 · DOI: 10.1021/jp406506d

6 AUTHORS, INCLUDING:

Yaoguang Rong
Huazhong University of Science and Technology
34 PUBLICATIONS **756** CITATIONS
SEE PROFILE

Xiong Li
École Polytechnique Fédérale de Lausanne
43 PUBLICATIONS **626** CITATIONS
SEE PROFILE

Hongwei Han
Huazhong University of Science and Technology
79 PUBLICATIONS **1,682** CITATIONS
SEE PROFILE

THE JOURNAL OF PHYSICAL CHEMISTRY C

Article

pubs.acs.org/JPCC

Improvement in Solid-State Dye Sensitized Solar Cells by *p*-Type Doping with Lewis Acid $SnCl_4$

Mi Xu, Yaoguang Rong, Zhiliang Ku, Anyi Mei, Xiong Li, and Hongwei Han*

Michael Grätzel Center for Mesoscopic Solar Cells, Wuhan National Laboratory for Optoelectronics, Huazhong University of Science and Technology, Wuhan, Hubei 430074, People's Republic of China

Supporting Information

ABSTRACT: The Lewis acid $SnCl_4$ is employed as a *p*-type dopant for 2,2′,7,7′-tetrakis(*N*,*N*-di-*p*-methoxyphenylamine)-9,9′-spirobifluorene (spiro-OMeTAD) for the solution process in solid-state dye sensitized solar cell. The UV−vis absorption spectra and time-resolved photoluminescence (PL) spectra are used to investigate the doping level of spiro-OMeTAD with a *p*-type dopant, indicating the strong molecular acceptor of $SnCl_4$. X-ray photoelectron spectra (XPS) exhibiting close energy shifts of the Fermi level toward HOMO are observed when adding Li salt or $SnCl_4$. A significant enhancement in fill factor of the photovoltaic devices, corresponding to the power conversion efficiency, is observed when doping with $SnCl_4$. This is attributed to the low charge transport resistance of the hole transport film and high hole injection efficiency from the hole transport material to the counter electrode.

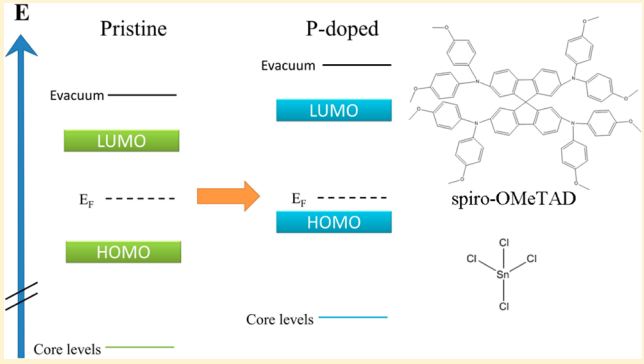

1. INTRODUCTION

Since U. Bach first reported an efficient solid state dye-sensitized solar cell (ss-DSC) with organic hole transport materials (HTM) 2,2′,7,7′-tetrakis(*N*,*N*-di-*p*-methoxyphenylamine)-9,9′-spirobifluorene (spiro-OMeTAD) in 1998,[1] intensive research has been carried out to accelerate the process of industrialization for this photovoltaic technology. Recently, a high efficiency exceeding 12% has been achieved employing organometal halide perovskite as light absorber and spiro-OMeTAD as hole transporting material (HTM).[2] Up to now, spiro-OMeTAD-based devices exhibit the highest efficiency for ss-DSC; however, there are still some obstacles during the fabrication process. Usually, the hole transfer occurring in organic semiconductors is described by a hopping mechanism between neighboring molecules, leading to a low hole mobility. The conductivity of the pristine organic semiconductor exhibits 2.0×10^{-5} S cm^{-1}, which is about 10-fold lower than that with *p*-type doping. And lithium bis(trifluoromethylsulfonyl)-imide (Li-TFSI) was found to be a crucial additive for spiro-OMeTAD, which would lead a significant increment of conductivity for the hole transport film.[3,4] Meanwhile, the electron injection efficiency from the LUMO of light absorber to the conduction band of TiO_2 was enhanced in the presence of lithium ions.[5] However, several researchers found that the doping with Li-TFSI was highly depended on the presence of oxygen atmosphere.[6,7] This ambient dependent process may lead to poor stability and reproducibility of the devices. Additionally, a recent work deduced that the lithium ions were consumed during the doping process, which would decrease the presence of lithium ions on the TiO_2 surface.[8]

Some works have been studied on enhancing the conductivity by *p*-type doping, and several kinds of organic molecule acceptor compounds have been developed for spiro-OMeTAD, such as $(p\text{-}BrC_6H_4)_3NSbCl_6$,[1] tris(2-(1H-pyrazol-1-yl)pyridine) cobalt(III),[4] and F4-TCNQ.[9] However, the applications of these organic materials are usually limited by their high volatility, high absorption in the visible region, or low production yield. Other inorganic *p*-dopants such as MoO_3 and WO_3 are usually applied by vacuum deposition techniques and exhibit poor solubility in organic solvents, which is not suitable for solution processes in the fabrication of ss-DSC. It remains a problem of great urgency to employ an available, efficient, and stable *p*-type dopant for spiro-OMeTAD.

It is well known that $SnCl_4$ has the unoccupied d orbital to accept electrons from hole transport material and consequently form charge-transfer complexes. Similar metal halides such as $SbCl_5$[10] and $FeCl_3$[11] have been developed as *p*-type dopants in organic light-emitting devices (OLEDs). Herein, we report a typical Lewis acid $SnCl_4$, which acts as the electron acceptor in spiro-OMeTAD for *p*-type doping with solution process and its application in ss-DSCs. Upon doping with a few molar rate of $SnCl_4$, the HTM film has a significant increase in conductivity, whereas the Fermi level moves toward the highest occupied molecular orbital (HOMO). Additionally, the influence of doping with $SnCl_4$ on the performance of ss-DSC was studied; the obvious improvement in fill factor (*FF*) can be attributed to

Received: July 1, 2013
Revised: October 8, 2013
Published: October 10, 2013

the lower charge transport resistance and higher hole injection efficiency from the HTM to the counterelectrode (CE).

2. EXPERIMENTAL SECTION

2.1. Device Fabrication. The devices based on a carbon counterelectrode were fabricated as follows:[12] Fluorine-doped tin-oxide (FTO) glass substrates with high transparency in the visible range were purchased from CSG Holding Co. Ltd. and etched with a laser before being cleaned ultrasonically with detergent, deionized water, and ethanol, respectively. A compact TiO_2 layer was deposited onto the patterned substrate by spray pyrolysis with oxygen as carrier gas, and then a 1.6 μm-thick TiO_2 (PASOLHPW-18NR) film was deposited by screen printing. After sintering at 500 °C, a 1.1 μm thick ZrO_2 (Tosoh zirconia powder TZ-3Y) layer and a 10 μm thick carbon (carbon black:graphite = 1:3.25) layer were printed layer by layer and then sintered at 400 °C. When the temperature had cooling down to 80 °C, the devices were then immersed into the dye D102 solution (0.5 mM in CH_3CN:*t*-BuOH (1:1)) and kept for eight hours. Spiro-OMeTAD was dissolved in chlorobenzene at a concentration of 0.15M, and then 0.12 M TBP was added. The dopant Li-TFSI and $SnCl_4$ were dissolved in acetonitrile before adding to the HTM solution at the certain molar ratio. After dyeing, the HTM solution was dropped onto the carbon layer and soaked for 2 min at room temperature, and then heated at 60 °C until the solvent evaporation.

2.2. Characteristics. UV–vis measurements were taken using a commercial spectrophotometer (Perkin-Elmer model Lambda 950) with an integrating sphere, and the samples were prepared in oxygen-free conditions before the test. Time-resolved photoluminescence data was collected by time-correlated single photon counting using FLS 920 (Edinburgh Instruments), and the samples were prepared by drop-casting on the glass slides in the ambient air and then dried at 60 °C. The excitation wavelength was chosen at 367 nm, and the monitoring wavelength was 445 nm. XPS measurements were carried out using the ESCALAB 250Xi spectrometer and a monochromatic Al Kα source. The spectrometer energy scale was calibrated using Au $4f_{7/2}$. Photocurrent density–voltage characteristics were taken with a Keithley 2400 sourcemeter under illumination with an Oriel solar simulator composed of a 1000 W xenon arc lamp and AM 1.5 G filters. Light intensity was calibrated with a normative silicon cell.

3. RESULTS AND DISCUSSION

Figure 1 shows the UV–vis absorption spectra of spiro-OMeTAD in chlorobenzene with the gradual contents of $SnCl_4$. As a comparison, the UV–vis absorption spectra of the highest content of $SnCl_4$ in chlorobenzene is presented. It could be found that the absorption spectrum rises ranging from 500 to 750 nm and an evident absorption peak appears at 522 nm when the $SnCl_4$ was added into spiro-OMeTAD solution. The peak position of signal is in good accordance with the typical result reported by U. B. Cappel et al.,[6] where oxidized spiro-OMeTAD is generated in the solution by *p*-type doping. However, the pure spiro-OMeTAD and the $SnCl_4$ solution have almost no absorption in the visible region. Obviously, the absorption peak could be attributed to the presence of cation radical of spiro-OMeTAD generated by the process of charge transfer between host and dopant. Normally, the first oxidation potential of spiro-OMeTAD has been found to be 0.68 V versus normal hydrogen electrode (NHE), whereas $SnCl_4$ has

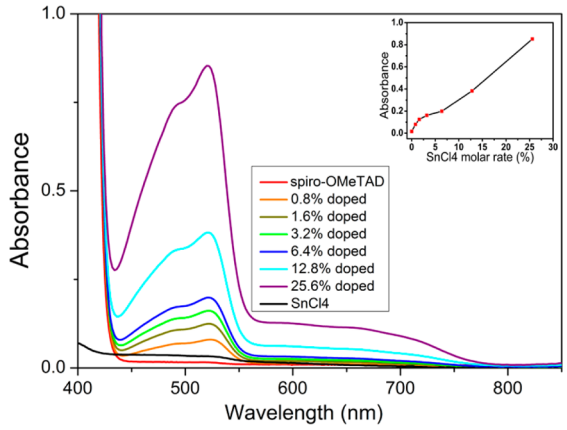

Figure 1. UV–vis absorption spectra of spiro-OMeTAD solution in chlorobenzene with the gradual contents of $SnCl_4$ and the highest content of $SnCl_4$ in the absence of spiro-OMeTAD in chlorobenzene. Inset: the absorbance at the absorption peak of 522 nm as a function of $SnCl_4$ content.

the oxidation potential 1.10 V vs NHE determined by cyclic voltammetry (CV). The potential gap of 0.42 V supplies the driving force for the charge transfer from the host to the dopant. The effective electron transfer from $SnCl_4$ molecular to spiro-OMeTAD could be illustrated in following equation:

$$2\text{spiro-OMeTAD} + Sn^{4+} \rightarrow 2\text{spiro-OMeTAD}^{+} + Sn^{2+}$$

Moreover, the height of the oxidized peak of spiro-OMeTAD in the UV–vis absorption spectrum corresponding to the concentration of oxidized spiro-OMeTAD improves approximately linearly with increasing content of $SnCl_4$ (see the inset in Figure 1). This observation suggested that $SnCl_4$ has strong ability to oxidize spiro-OMeTAD, and the oxidation process is independent of ambient air varying from Li-salt-doping. Therefore, $SnCl_4$ is able to accept electrons from spiro-OMeTAD and form a charge transfer complex in the solid film, consequently generating numerous free holes as a *p*-type dopant.

It is well-known that *p*-type doping could occur via charge transfer from the HOMO of spiro-OMeTAD to the lowest unoccupied molecular orbital (LUMO) (or the conduct band) of the dopant as the nonradiative process, which can be observed by time-resolved photoluminescence (PL) spectra. In this charge transfer complex, the major nonradiative process is intermolecular charge transfer from the host to the dopant, which may lead to the quenching of photoluminescence. Meanwhile, the photoluminescence spectra of spiro-OMeTAD and $SnCl_4$ in chlorobenzene (Supporting Information Figure S1) indicates $SnCl_4$ itself has negligible photoluminescence competing with spiro-OMeTAD in this complex. Figure 2a shows the PL decay curve of the pristine and spiro-OMeTAD film doped with *p*-type dopants. The experiment was performed with an excitation laser wavelength of 367 nm and monitored at 445 nm emission. In the absence of additives, the laser excited the spiro-OMeTAD molecule to the excited state. Therefore, fluorescence occurs when the excited electron relaxes to its ground state. In the film containing the *p*-type dopant, an obvious photoluminescence quenching was observed, which is caused by the dopant quench the HTMs excitonic emission efficiently. With the increase of doping level with Li salt, the faster quenching and shorter lifetime of excited state were represented, indicating the quickened rate of charge

dx.doi.org/10.1021/jp406506d | J. Phys. Chem. C 2013, 117, 22492–22496

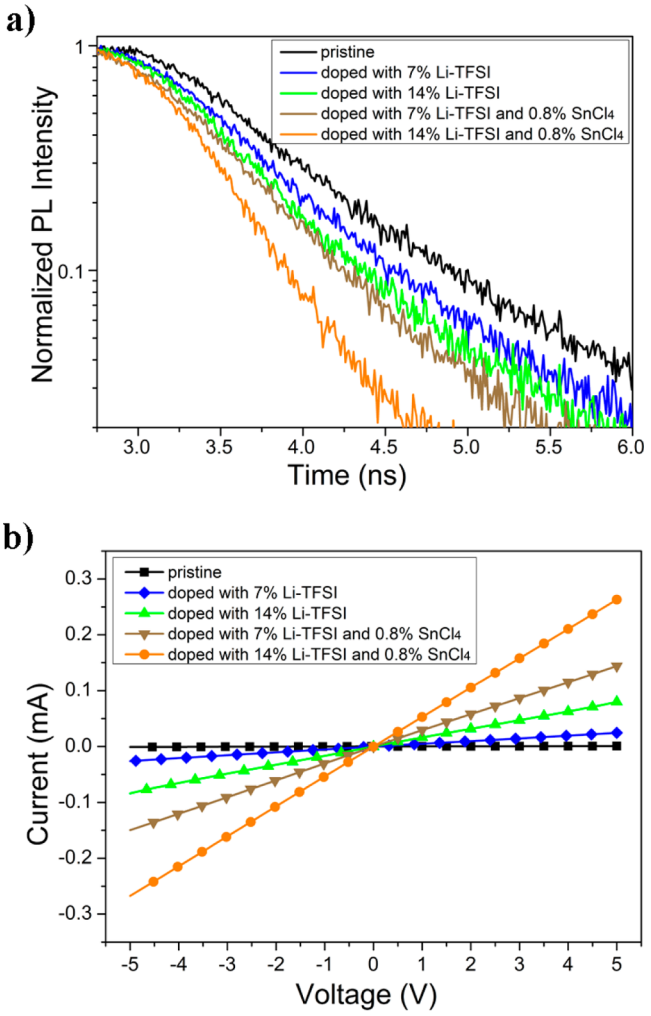

Figure 2. (a) PL decay curve and (b) I–V curves of CE/HTM/CE devices for the pristine and spiro-OMeTAD film doped with *p*-type dopant.

transfer from spiro-OMeTAD to Li salt. Interestingly, a more significant PL quenching was performed for the spiro-OMeTAD film once doped with $SnCl_4$. This result is consistent well with the UV–vis absorption spectra data and suggests that conspicuous charge transfer processes occur from spiro-OMeTAD to $SnCl_4$, which would increase the hole mobility of the HTM film. Herein, it is notable that very low $SnCl_4$ doping concentration less than 1% molar rate provides a higher charge transfer efficiency compared to that of the Li salt doping at a common rate. It has been mentioned that plenty of factors, such as the energy levels of host and dopant, a phase separation between matrix and dopant, and the occurrence of charge trapping, have been considered to lower the doping efficiency,[13] which might limit the charge transfer efficiency of Li salt doping.

In order to analyze the different of *p*-type dopants of Li salt and $SnCl_4$ in spiro-OMeTAD, the mesoscopic carbon electrode/HTMs/mesoscopic carbon electrode devices were fabricated. The current–voltage (I–V) curves of the devices with (A) spiro-OMeTAD, (B) spiro-OMeTAD doped with 7% Li-TFSI, (C) spiro-OMeTAD doped with 14% Li-TFSI, (D) spiro-OMeTAD doped with 7% Li-TFSI/0.8% $SnCl_4$, and (E) spiro-OMeTAD doped with 14% Li-TFSI/0.8% $SnCl_4$ are presented in Figure 2b. Obviously, the currents are linearly dependent on the voltage from −5 V to 5 V, indicating ohmic contact in the devices. It could be found that the slope of the I–V curve follows a trend of (E) > (D) > (C) > (B) > (A), which indicates that the conductivity of HTM could be improved through doping and the high conductivity of HTM could be obtained with the high concentration of dopant. Moreover, a significant improvement in conductivity is observed when a small quantity of $SnCl_4$ is added to the spiro-OMeTAD doped with Li salt film, which agrees well with the photoluminescence result. On the other hand, the conductivity of different concentrations of $SnCl_4$ in spiro-OMeTAD were also measured (Supporting Information Figure S2), which shows the gradual improvement with the increment of $SnCl_4$.

In order to investigate the effect of energy level shifts when Li-TFSI and $SnCl_4$ were added into spiro-OMeTAD, X-ray photoelectron spectra (XPS) of the pristine spiro-OMeTAD film, the spiro-OMeTAD film doped with Li salt, and the spiro-OMeTAD film doped with $SnCl_4$ were characterized with the assistance of the ESCALAB 250Xi spectrometer, which is presented in Figure 3a. It could be found that for the pristine

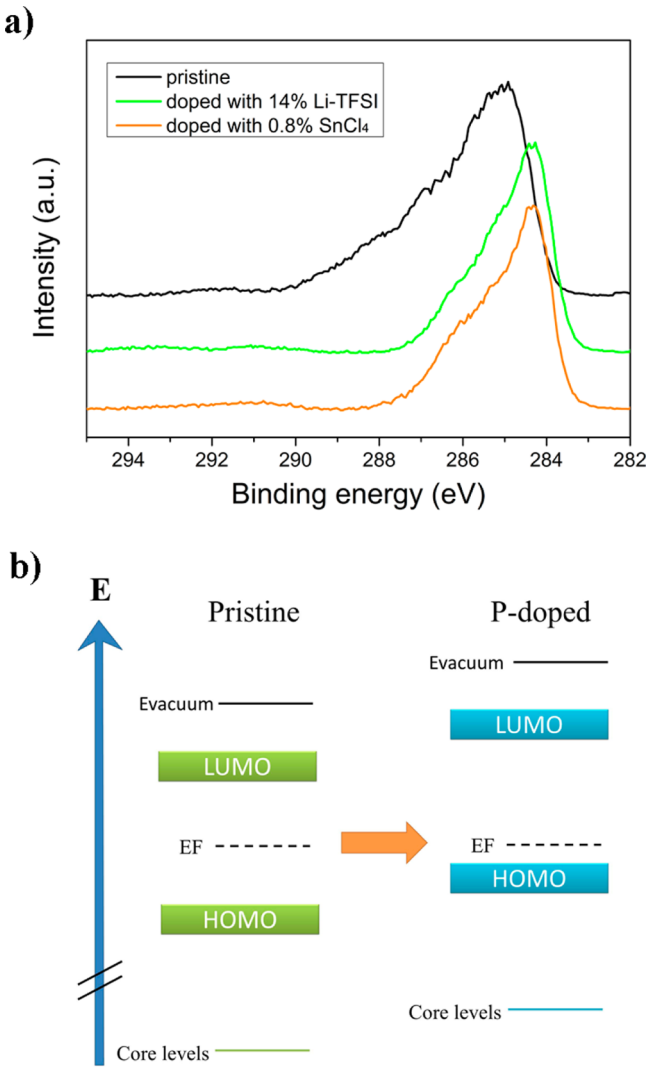

Figure 3. (a) The C 1s core level spectra of pristine spiro-OMeTAD film and spiro-OMeTAD film with *p*-type dopant. (b) Energy level scheme for the undoped and doped states for spiro-OMeTAD.

dx.doi.org/10.1021/jp406506d | J. Phys. Chem. C 2013, 117, 22492–22496

material, the carbon C 1s signal consists of a single peak with the maximum located 285.2 eV. When adding Li salt into spiro-OMeTAD, the C 1s peak shifted toward lower binding energy of 284.42 eV. Meanwhile, the spiro-OMeTAD film doped with $SnCl_4$ shows the approximate value of 284.43 eV. Because the identical shifts of the HOMO of spiro-OMeTAD and C1s core level were observed during *p*-type doping; hence, assuming a constant energy distance between the core level and the HOMO of the HTM,[14] the energy shifts of C1s core level on the XPS plot are directly related to the corresponding the shifts of the Fermi level toward the HOMO in spiro-OMeTAD.[15] Figure 3b shows the energy level scheme for the undoped and doped state of spiro-OMeTAD. Interestingly, close energy downward shifts of around 0.8 eV for C 1s core level are observed with doping $SnCl_4$ or Li salt. In general, this approach of Fermi level toward HOMO would lower the hole injection barrier, which will facilitate forming ohmic contact at the interface of the counter electrode and, hence, increase the short circuit current density (J_{sc}) and *FF* of the photovoltaic devices. This result suggests that the two additives play a similar role in energy level alignment of a dopant/host blend and should present a considerable ability of $SnCl_4$ for *p*-type doping.

In order to understand the effect of $SnCl_4$-doping on the performance of ss-DSCs, three types of devices based on spiro-OMeTAD doped with (A) $SnCl_4$ of 0.8%, (B) Li salt of 14%, and (C) Li salt of 14% and $SnCl_4$ of 0.8% are fabricated. The photocurrent density−voltage (*J*−*V*) characteristics of the ss-DSCs with spiro-OMeTAD doped with different dopants are presented in Figure 4. It could be found that device A without

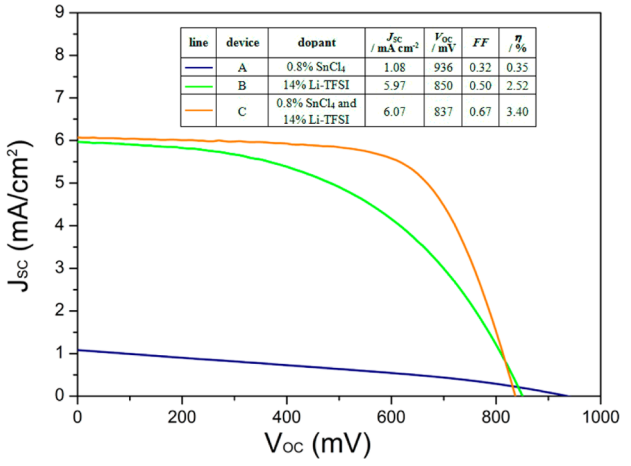

Figure 4. J-V characteristics of the devices with *p*-type doping. (A) HTMs doped with $SnCl_4$ of 0.8%. (B) HTMs doped with Li-TFSI of 14%. (C) HTMs doped with Li-TFSI of 14% and $SnCl_4$ of 0.8%.

Li salt exhibits an open-circuit voltage (V_{OC}) of 936 mV, J_{SC} of 1.08 mA/cm^2, *FF* of 0.32, and power conversion efficiency (η) of 0.35%. The poor performance is reasonable because the Li^+ lays a key role in the charge dynamics at the TiO_2/dye/HTMs interface, where a significant acceleration of the electron injection from the oxidized dye to the photo anode[5,16] and longer injected electron lifetime[7] were observed in the presence of Li^+. Upon the addition of Li-TFSI, η of the device B has clearly improved to 2.52%, whereas V_{OC} decreases to a lower value of 850 mV. The decline of V_{OC} is caused by the downward shift of the TiO_2 conduction band when Li^+ was added, which is similar to another doping process in the dye/TiO_2/FTO complex. Compared to device B, device C based on spiro-OMeTAD doped with Li salt of 14% and $SnCl_4$ of 0.8% has a significant increment in *FF* from 0.50 to 0.67; hence, η increases from 2.52% to 3.40%, which can be attributed to the higher charge mobility and, therefore, lower charge transport resistance of the HTMs film and higher hole injection efficiency. However, a slightly downward of V_{OC} from 850 to 837 mV is observed when $SnCl_4$ was introduced into spiro-OMeTAD doped with Li salt of 14%, where the approaches of Fermi level toward HOMO show similar results with the two additives. This phenomenon is probably caused by the accumulation of holes near the sensitized junction corresponding to the increased recombination rate between holes and electrons in the conduction band when doping at high levels, which can be verified by the dark current (Supporting Information Figure S3). As a result, $SnCl_4$ doping could significantly improve the performance of the ss-DSCs by enhancing the doping level of hole conductor.

4. CONCLUSIONS

In summary, we have applied solution-processed Lewis acid $SnCl_4$ as a *p*-type dopant in the spiro-OMeTAD matrix and investigated its application in ss-DSC devices. The UV−vis absorption spectra and time-resolved PL spectra demonstrate that a low level of $SnCl_4$ could significantly enhance the doping level of HTM and consequently increase the hole mobility and conductivity. Meanwhile, close energy shifts of the Fermi level toward HOMO are observed when adding Li-salt or $SnCl_4$, showing the considerable potential of metal halides in *p*-type doping. The photovoltaic characteristic of the ss-DSC with $SnCl_4$ doping exhibits significant enhancements in *FF*. Further investigation will focus on replacing the Li−TFSI to avoid the decline of V_{OC}.

■ ASSOCIATED CONTENT

Ⓢ Supporting Information

The photoluminescence spectra of spiro-OMeTAD and $SnCl_4$ in chlorobenzene (Figure S1), the conductivity measurements of different concentrations of $SnCl_4$ in spiro-OMeTAD (Figure S2), the dark J-V curve of the devices with and without $SnCl_4$ doping (Figure S3). This information is available free of charge via the Internet at http://pubs.acs.org.

■ AUTHOR INFORMATION

Corresponding Author

*H. Han. E-mail: hongwei.han@mail.hust.edu.cn. Phone: +86 27 8779 3027.

Notes

The authors declare no competing financial interest.

■ ACKNOWLEDGMENTS

The authors acknowledge the financial support by the Ministry of Science and Technology of China (863, no. SS2013AA50303), the National Natural Science Foundation of China (grant no. 61106056), the fundamental Research Funds for the Central Universities (HUSTNY022), and Scientific Research Foundation for Returned Scholars, Ministry of Education of China.

■ REFERENCES

(1) Bach, U.; Lupo, D.; Comte, P.; Moser, J. E.; Weissortel, F.; Salbeck, J.; Spreitzer, H.; Gratzel, M. Solid-State Dye-Sensitized

Mesoporous TiO_2 Solar Cells with High Photon-to-Electron Conversion Efficiencies. *Nature* **1998**, *395*, 583−585.
(2) Lee, M. M.; Teuscher, J.; Miyasaka, T.; Murakami, T. N.; Snaith, H. J. Efficient Hybrid Solar Cells Based on Meso-Superstructured Organometal Halide Perovskites. *Science* **2012**, *338*, 643−647.
(3) Snaith, H. J.; Grätzel, M. Enhanced Charge Mobility in a Molecular Hole Transporter Via Addition of Redox Inactive Ionic Dopant: Implication to Dye-Sensitized Solar Cells. *Appl. Phys. Lett.* **2006**, *89*, 262114.
(4) Burschka, J.; Dualeh, A.; Kessler, F.; Baranoff, E.; Cevey-Ha, N.-L.; Yi, C.; Nazeeruddin, M. K.; Grätzel, M. Tris(2-(1h-Pyrazol-1-Yl)Pyridine)Cobalt(III) as *p*-type Dopant for Organic Semiconductors and Its Application in Highly Efficient Solid-State Dye-Sensitized Solar Cells. *J. Am. Chem. Soc.* **2011**, *133*, 18042−18045.
(5) Furube, A.; Katoh, R.; Hara, K.; Sato, T.; Murata, S.; Arakawa, H.; Tachiya, M. Lithium Ion Effect on Electron Injection from a Photoexcited Coumarin Derivative into a TiO_2 Nanocrystalline Film Investigated by Visible-to-IR Ultrafast Spectroscopy. *J. Phys. Chem. B* **2005**, *109*, 16406−16414.
(6) Cappel, U. B.; Daeneke, T.; Bach, U. Oxygen-Induced Doping of Spiro-MeOTAD in Solid-State Dye-Sensitized Solar Cells and Its Impact on Device Performance. *Nano Lett.* **2012**, *12*, 4925−4931.
(7) Yang, L.; Xu, B.; Bi, D.; Tian, H.; Boschloo, G.; Sun, L.; Hagfeldt, A.; Johansson, E. M. J. Initial Light Soaking Treatment Enables Hole Transport Material to Outperform Spiro-OMeTAD in Solid-State Dye-Sensitized Solar Cells. *J. Am. Chem. Soc.* **2013**, *135*, 7378−7385.
(8) Abate, A.; Leijtens, T.; Pathak, S.; Teuscher, J.; Avolio, R.; Errico, M. E.; Kirkpatrik, J.; Ball, J. M.; Docampo, P.; McPherson, I.; et al. Lithium Salts as "Redox Active" *p*-type Dopants for Organic Semiconductors and Their Impact in Solid-State Dye-Sensitized Solar Cells. *Phys. Chem. Chem. Phys.* **2013**, *15*, 2572.
(9) Chen, D.-Y.; Tseng, W.-H.; Liang, S.-P.; Wu, C.-I.; Hsu, C.-W.; Chi, Y.; Hung, W.-Y.; Chou, P.-T. Application of F4TCNQ Doped Spiro-MeOTAD in High Performance Solid State Dye Sensitized Solar Cells. *Phys. Chem. Chem. Phys.* **2012**, *14*, 11689.
(10) Ganzorig, C.; Fujihira, M. Improved Drive Voltages of Organic Electroluminescent Devices with an Efficient *p*-type Aromatic Diamine Hole-Injection Layer. *Appl. Phys. Lett.* **2000**, *77*, 4211.
(11) Endo, J.; Matsumoto, T.; Kido, J. Organic Electroluminescent Devices with a Vacuum-Deposited Lewis-Acid-Doped Hole-Injecting Layer. *Jpn. J. Appl. Phys.* **2002**, *41*, L358−L360.
(12) Xu, M.; Liu, G. H.; Li, X.; Wang, H.; Rong, Y. G.; Ku, Z. L.; Hu, M.; Yang, Y.; Liu, L. F.; Liu, T. F.; et al. Efficient Monolithic Solid-State Dye-Sensitized Solar Cell with a Low-Cost Mesoscopic Carbon Based Screen Printable Counter Electrode. *Org. Electron.* **2013**, *14*, 628−634.
(13) Hamwi, S.; Meyer, J.; Winkler, T.; Riedl, T.; Kowalsky, W. *p*-type Doping Efficiency of MoO_3 in Organic Hole Transport Materials. *Appl. Phys. Lett.* **2009**, *94*, 253307.
(14) Hock, R.; Mayer, T.; Jaegermann, W. *p*-type Doping of Spiro-MeOTAD with WO_3 and the Spiro-MeOTAD/WO_3 Interface Investigated by Synchrotron-Induced Photoelectron Spectroscopy. *J. Phys. Chem. C* **2012**, *116*, 18146−18154.
(15) Schölin, R.; Karlsson, M. H.; Eriksson, S. K.; Siegbahn, H.; Johansson, E. M. J.; Rensmo, H. Energy Level Shifts in Spiro-OMeTAD Molecular Thin Films When Adding Li-TFSI. *J. Phys. Chem. C* **2012**, *116*, 26300−26305.
(16) Bai, Y.; Zhang, J.; Wang, Y.; Zhang, M.; Wang, P. Lithium-Modulated Conduction Band Edge Shifts and Charge-Transfer Dynamics in Dye-Sensitized Solar Cells Based on a Dicyanamide Ionic Liquid. *Langmuir* **2011**, *27*, 4749−4755.